8-30-2019

Characterization of Cerium (III) Ion Binding to Surface-Immobilized EF-Hand Loop I of Calmodulin

MingYuan Xu
Case Western Reserve University

Zihang Su
Case Western Reserve University

Julie N. Renner
Case Western Reserve University, julie.renner@case.edu

Author(s) ORCID Identifier:

MingYuan Xu

Zihang Su

Julie N. Renner

Characterization of cerium (III) ion binding to surface-immobilized EF-hand loop I of calmodulin

*MingYuan Xu, Zihang Su, and Julie N. Renner**

Department of Chemical and Biomolecular Engineering, Case Western Reserve University, Cleveland, OH 44106

* Corresponding Author: Email: jxr484@case.edu, Phone: 216-368-2905

Abstract

Cerium has a wide range of current and emerging applications, and the binding of cerium ions to solid substrates is important for cerium recovery, or in advanced material synthesis. In this study, we investigate the affinity of a surface-bound peptide derived from the EF-hand loop I of calmodulin for cerium (III) ions and compare the results to a scrambled control. Results obtained via quartz crystal microbalance with dissipation are used to estimate the dissociation constant between the EF-hand loop I peptide and cerium (III) ions (1.3 ± 0.1 μM), which is comparable with other dissociation constants measured for EF-hand peptides and cerium ions in solution reported in literature (0.95-5.8 μM). Circular dichroism also suggests that the peptide binds to cerium (III) ions in solution, and undergoes a secondary structural change upon binding. Overall, this study shows that EF-hand loop peptides are capable of binding cerium (III) ions in solution and when attached to a solid substrate.

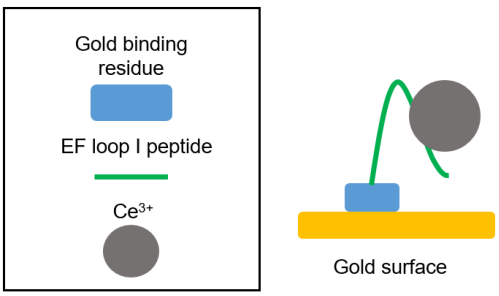

Keywords

affinity peptide, cerium, calmodulin, EF-hand motif

1 Introduction

Cerium is the most abundant member of the lanthanide chemical series, and is used in many applications including in automotive catalytic converters,[1] in flow battery designs,[2, 33] as a polishing media,[4] and as a potential phosphor in light emitting diodes.[4, 5] Cerium-based thin-film materials[6, 7] as well as nanoparticles[8, 9] have been explored for applications in sensing, biomedicine, agriculture and nutrient recovery.[10] Thus, the binding of cerium ions to solid substrates could be potentially useful for cerium recovery, or in material synthesis.

Affinity peptides have been proposed as promising ways to recover metal ions,[11] and direct nanomaterial and film formation.[12, 13] EF-hand sequences which consist of helix-loop-helix motifs, bind to calcium ions in nature,[14] but are also well-known to have affinity for lanthanide ions.[15] While many studies have investigated EF-hand peptides for binding lanthanide ions in solution,[16-22] including cerium (IV) ions (Ce^{4+}),[16] only a few have specifically investigated cerium (III) ions (Ce^{3+}).[23, 24] Additionally, while some studies have immobilized peptides on gold surfaces for lanthanide binding,[25-27] the effect of immobilizing the peptides to solid substrates on the binding affinity is often not quantified. This binding information is useful for material design.

To understand the capacity of EF-hand peptides to bind to Ce^{3+} when immobilized, a sequence derived from EF-hand loop I of calmodulin is explored. In work by Ye *et al.*, four EF-hand loops from calmodulin were grafted into a scaffold protein to study calcium and lanthanide binding. They found that site I (DKDGDGTITTKE) has the highest affinity for calcium and lanthanide ions and thus, this sequence serves as the basis for this study, and was modified to bind to a solid surface. To detect the interaction between the peptide and Ce^{3+} in solution, circular dichroism (CD) is employed and isothermal titration calorimetry (ITC) is used to confirm the results. To understand the binding of the peptide when immobilized to gold, a quartz crystal microbalance with dissipation (QCM-D) is utilized, in combination with a Scatchard analysis. Binding constants are obtained and compared to literature. Overall, this study provides fundamental binding information that can be utilized in future peptide-based material designs.

2 Materials and Methods

2.1 Materials

Cerium (III) chloride ($CeCl_3$ 99.9%) heptahydrate was purchased from Sigma-Aldrich. Deionized water (DI water) was used throughout the study and was obtained from a mixed bed deionizer tank of Western Reserve Water System (1-10 megohm). Ammonium hydroxide solution (NH_4OH, 30%) was purchased from Alfa Aesar. Sodium dodecyl sulfate (SDS, $C_{12}H_{25}NaO_4S$, 99%) was purchased from Hoefer. Hydrogen peroxide solution (H_2O_2, 25%) was purchased from Sigma Aldrich. Nitrogen

(N_2) gas (>99%) was obtained from Airgas.

2.2 Peptide design

The lanthanide binding sequence utilized was derived from loop I of calmodulin (DKDGDGTITTKE), previously shown to have the highest lanthanide affinity compared to the other three potential binding sites found in the protein.[17] This sequence was randomly rearranged to create a scrambled control (TDGGDTDKTEIK). This peptide was previously suspected to bind to cerium ions in solution based on a preliminary ITC and CD experiment [Yi Z. unpublished results], and thus served as the basis for this work. Both the EF-hand loop I peptide and the scrambled control were modified with a cysteine (C) residue at the N-terminus to covalently attach the peptide to gold via a thiol bond. The terminal cysteine was separated from the rest of the peptide by three glycine residues as previous work has shown reduced ion binding affinity in scaffold proteins without the spacers.[28] The ends of both peptides were acylated and amidated to increase peptide stability by preventing degradation, and to mimic the natural sequence. **Figure 1** shows the full sequence of each peptide designed for this study. Peptides were ordered from GenScript at a purity of >90%.

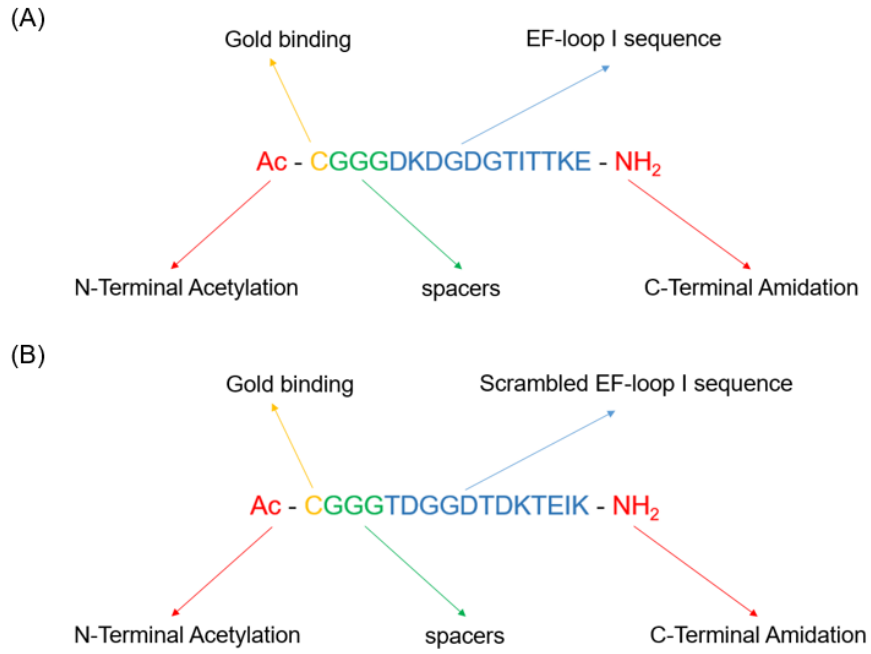

Figure 1. Peptide designs to study binding of Ce^{3+} when peptides are surface-bound, featuring a lanthanide-binding sequence (A, shown in blue) and scrambled control (B, shown in bue). Each peptide contains a cysteine residue (yellow), as a means to covalently bind to gold, spacer residues (green), and N-terminal acetylation and C-terminal amidation (red).

2.3 Circular Dichroism (CD)

Circular dichroism (CD, Jasco J-815) was used to evaluate the secondary structure of the peptides in the presence and absence of $CeCl_3$ in solution. Nitrogen gas was used to purge the instrument for 30 minutes before experiments. The baseline consisted of DI water. Spectrum were collected at 20ºC on 250 µL of solution from 190-260 nm with a path length of 0.1 nm, 1.00 nm bandwidth, a scanning speed of 20 nm/min and a 0.5

nm data pitch. The data are represented as the average of 5 accumulations. The concentration of peptide solutions was 150 μg/ml, and the molar ratio between Ce^{3+} and peptide was 1:1 such that the final $CeCl_3$ heptahydrate concentration was 35 μg/ml (both molar concentrations were 94 μM, see **Table S1**).

2.4 Isothermal titration calorimetry (ITC)

Isothermal titration calorimetry (ITC) was used to confirm the binding of Ce^{3+} in solution. Estimates of the equilibrium disassociation constant (K_D) and the enthalpy (ΔH), entropy (ΔS) and Gibbs free energy (ΔG) of interaction were obtained by fitting integrated heat curves with a one set of sites model[29] using a Microcal ITC 200 with Origin software via nonlinear least squares fitting, and using equations found in Supplemental Information. $CeCl_3$ was titrated into the peptide solutions. A 7.5 mg/mL solution (20 mM) $CeCl_3$ solution was titrated into 280 μL of a 0.8 mg/mL peptide solution (0.5 mM) in 19 does of 2.1 μL injections at 25ºC. The first injection volume was 0.8 μL and was removed before the model fitting. A baseline was obtained without peptide and subtracted prior to model fitting to account for heat changes due to mixing.

2.5 Quartz Crystal Microbalance with Dissipation (QCM-D)

A quartz crystal microbalance with dissipation (QCM-D, Biolin, Gothenburg, Sweden) flow module was used to measure mass variation with time by detecting the change in frequency of gold-coated resonating quartz crystal sensor (QSX301, 5MHz, Biolin Scientific) exposed to solutions of peptide and $CeCl_3$. Before experiments, the sensor

was treated by an ultraviolet (UV) light ozone generator (Novascan, Boone, Iowa) for 15 minutes and placed in 21 ml 75ºC piranha buffer (5:1:1 mixture of DI water, 30% hydrogen peroxide and 25% ammonium hydroxide) for 5 minutes. After heating, the sensor was rinsed with DI water and dried with nitrogen gas. The dry sensor was treated with the ultraviolet (UV) light ozone generator for an additional 15 minutes. The QCM-D flow module and tubing were cleaned using a dummy sensor with 20 ml of 2% SDS and followed by 100 mL DI water rinse. The clean gold sensors were placed in the clean QCM-D flow module for experiments. A stable baseline was established by running DI water through the flow module at 150 µL/min until there was no significant shift in frequency (below 0.5 Hz in 10 min). After establishing the baseline, 10 µg/ml peptide solution was sent through the flow module at 150 µL/min. After equilibrium was established, DI water was introduced to rinse any loosely-bound peptide. A solution of $CeCl_3$ heptahydrate was added to the module in increasing concentrations (0.5, 1, 2, 5, 10 and/or 100 µg/ml in DI water) after equilibrium was reached for each step. The pH of all solutions was 5.4 ± 0.2. The fifth overtone was used in all data analysis. The procedure was performed three separate times with the EF-hand loop I peptide to derive an equilibrium disassociation constant (K_D) using Scatchard analysis (see Supplemental Information), and compared to one run with the scrambled control. Peptide layer analysis was conducted with four samples.

2.6 Statistical Analysis

Estimates provided in **Table 1** were obtained from Microcal ITC 200 with Origin

software via nonlinear least squares fitting of ITC data. Parameter estimates are represented as parameter ± standard error. Data in **Table 2** are represented as the mean ± standard deviation. Means and standard deviations were calculated using Excel. A simple linear regression was performed on the equilibrium QCM-D binding data to obtain the Scatchard plot shown in **Figure 5**. The analysis was performed using JMP. Parameter estimates from the Scatchard analysis are represented as parameter ± standard error.

2.7 Solution pH and Concentration

Testing was performed in DI water to avoid any effects (mass adsorption) from buffer components on binding during QCM-D measurements.[30] To remain consistent with QCM-D, DI water was utilized for CD and ITC as well. The pH of all peptide and cerium solutions in DI water was measured to be 5.4 ± 0.2. We note that the net charge of the peptide is expected to be similar at neutral pH (pH 7) versus pH 5.4 (**Figure S1**), though the effect of binding at neutral pH was not part of this study. Additionally, we expect the Ce^{3+} ion will be stable in the pH range tested, according to a recent version of the Pourbaix diagram.[31] All solution concentrations are given as µg/mL and molar concentrations can be found in **Table S1**.

3 Results and Discussion

3.1 Peptide secondary structure analysis in DI water using circular dichroism (CD)

The secondary structures of the EF-hand loop I peptide (**Figure 2A**) and the scrambled

peptide (**Figure 2B**) were measured in DI water alone, and in the presence of $CeCl_3$ using CD. It has been previously observed for another loop peptide (DKDGDGYISAAE) that the secondary structure will change when exposed to lanthanum ions.[18, 32] Thus, the CD experiments also serve as an initial screen to detect binding of Ce^{3+} in solution. **Figure 2** shows the representative CD data, where both peptides have a strong negative peak at 198 nm and a weak negative shoulder at ~220 nm. After mixing the same molar concentration of Ce^{3+} into peptide solutions, the scrambled peptide spectra did not change. However, mixing the Ce^{3+} with the EF-hand loop I peptide caused the shoulder at ~220 nm to become more negative, as observed in similar peptides.[18] The observed shift to a more negative shoulder when the peptide is exposed to a lanthanide species has also been interpreted as increase in alpha helix content.[19] **Figure S2A-F** contain repeats of these experiments where similar trends are observed.

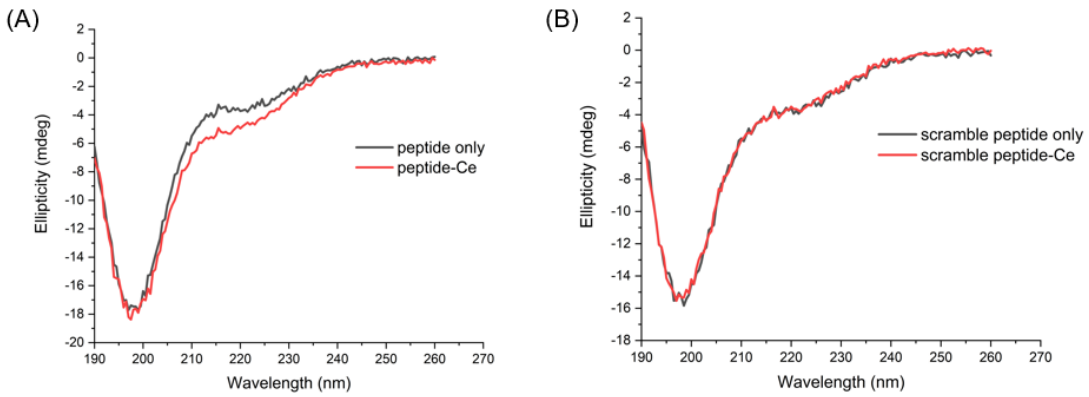

Figure 2. CD spectra of (A) EF-hand loop I peptide in DI water (black line) and in the presence of the same molar concentration of Ce^{3+} (red line), and (B) scrambled EF-hand loop I peptide in DI water (black line) and in the presence of the same molar concentration of Ce^{3+} (red line).

3.2 Isothermal titration calorimetry (ITC) analysis

ITC experiments were performed to determine the thermodynamic parameters (K_D, ΔH, ΔS, and ΔG) of the interaction between the peptide and Ce^{3+} in solution. **Figure 3A** shows a titration of EF-hand loop I peptide with $CeCl_3$ in DI water. The binding is endothermic, and representative in nature of other ITC experiments with calmodulin loop peptides and lanthanides.[22] **Figure 3B** shows the integrated titration curve plotted against molar ratio of ligand to peptide, with the background subtracted. The integrated data is fit with the one-set-of-sites model to derive thermodynamic parameters (**Figure S3**) where the solid line represents the model obtained via nonlinear least squares fitting.

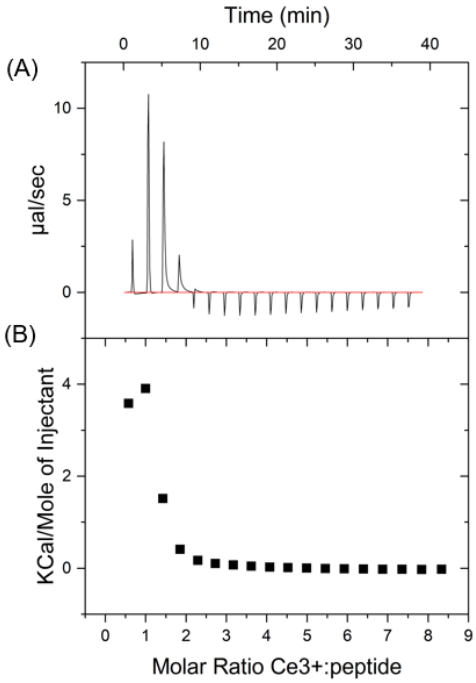

Figure 3. ITC for the EF-hand loop I peptide (CGGGDKDGDGTITTKE) with cerium (III) chloride where (A) the heat change with each injection is measured with time and (B) integrated to find the heat change per mole of Ce^{3+} and plotted against molar ratio

of Ce^{3+}.

Table 1 shows the results of fitting a one set of sites model to the data. The positive enthalpy and entropy value suggest the binding process under these conditions is entropy driven. It is generally thought that the binding of calcium ions to these EF-hand sequences is driven by an increase in solvent (water) entropy.[33] These values are comparable to other values obtained via ITC on a calmodulin-derived loop peptide (DKDGDGYISAAE) which were estimated to be $K_D = 5.3 \pm 0.6$ μM and $\Delta H = 2100 \pm 100$ cal/mol with lanthanum (III) ions.[22]

Table 1. Estimates of thermodynamic parameters derived from ITC experiment for binding of the EF-hand loop I peptide (CGGGDKDGDGTITTKE) peptide with Ce^{3+}. Error is derived from the nonlinear curve fitting. The K_D is 2.9 μM.

K_A (M^{-1})	ΔH (cal/mol)	ΔS (cal/mol/K)	ΔG (cal/mol)
340000 ± 280000	3900 ± 100	38	-7500 ± 200

3.3 Quartz crystal microbalance with dissipation (QCM-D) binding analysis

Binding analysis of the peptides to a gold surface and surface-bound peptides to Ce^{3+} was conducted via QCM-D.[34-36] **Figure 4** shows a representative QCM-D run (additional QCM-D runs shown in **Figure S4**).

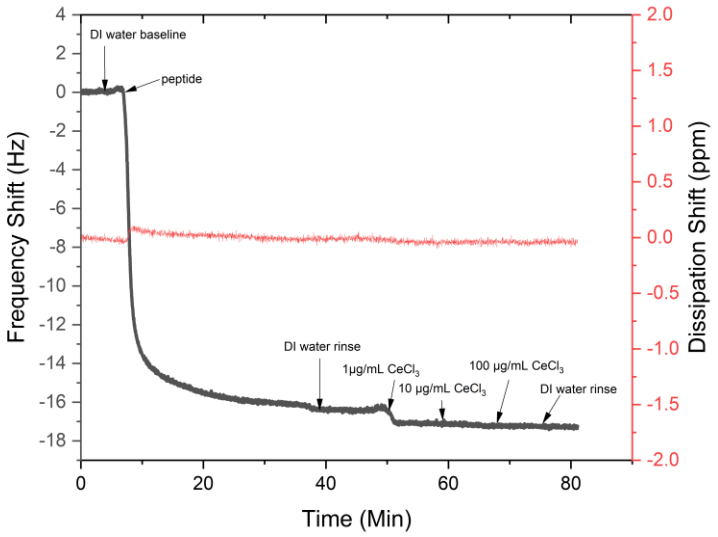

Figure 4. QCM-D monitoring of frequency (black) and dissipation (red) with time shows that gold-bound EF-hand loop peptide can bind with Ce^{3+}. Except the baseline, arrows in the image indicate when a new solution was added to the flow module. Concentrations shown are for $CeCl_3$ heptahydrate.

DI water served as the baseline, and also as the carrier for peptides and Ce^{3+}. Once a stable baseline was established, a peptide solution was introduced and the frequency shifted negative, which indicated that the mass increased on the gold sensor. The dissipation was also monitored, and no significant shifts were observed, indicating that the layers formed were rigid, and could be modeled using the Sauerbrey equation (see Supplemental Information for details). After equilibrium was established, DI water was used to rinse any loosely bound peptide from the surface to ensure a stable system prior to adding Ce^{3+}. The stable peptide layer was analyzed to determine the mass loading and thickness (**Table 2**, see Supplemental Information for calculations). The EF-hand loop I peptide and the scrambled peptide form comparable layers.

Table 2. QCM-D analysis of peptide layers on gold. Error bars are the standard deviation from measurements of four separate samples of EF-hand Loop I Peptide (n=4).

	Hydrated Peptide Loading (ng/cm^2)	**Hydrated Peptide Layer Thickness (nm)**
EF-hand Loop I Peptide	280 ± 40	2.5 ± 0.3
Scrambled Peptide	290	2.4

Once the peptide layer was established, binding of Ce^{3+} was analyzed by flowing solutions of cerium (III) chloride at different concentrations past the peptide-functionalized sensor. As seen in **Figure 4**, after the sensor was exposed to1 μg/mL $CeCl_3$ heptahydrate, a negative frequency shift was observed. Subsequent exposure to higher concentrations did not result in significant negative frequency shifts, indicating the peptides were nearly saturated after exposure to 1 μg/mL. This is especially clear in the test shown in **Figure S4A** where 0.5 μg/mL concentration is used prior to 1 μg/mL. To test if the frequency shift was due to the presence of the EF-hand loop I peptide and not the gold surface, a control test without peptide was conducted (**Figure S**5) where no frequency shifts were observed. Another control test with a scrambled peptide was conducted (**Figure S6**), which showed similar peptide binding behavior with a stable negative frequency shift similar to that of the EF-hand loop peptide. When the $CeCl_3$ solution was added into the system, a lower frequency change was observed (~0.3 Hz vs. ~1 Hz) for sensors with immobilized scramble peptide, corroborating the CD results indicating that the sequence of the peptide is important for binding Ce^{3+}.

3.4 Scatchard analysis of the QCM-D data

The data obtained from QCM-D in **Figure 4** and **Figure S4** can be used to conduct a Scatchard analysis[34-37] and estimate an equilibrium binding constant for the surface-bound EF-hand loop I peptide. **Figure 5** shows a Scatchard plot using the QCM-D data from **Figure 4** with an outlier removed. **Figure S7** shows the Scatchard plot with all of the data, and the normal quantile plot which was used to identify outliers. **Tables S2-S4** show the statistical analysis of the linear fit for this data, and parameter estimates. The analysis suggests the linear fit is significant. All Scatchard calculation details can be found in Supplemental Information.

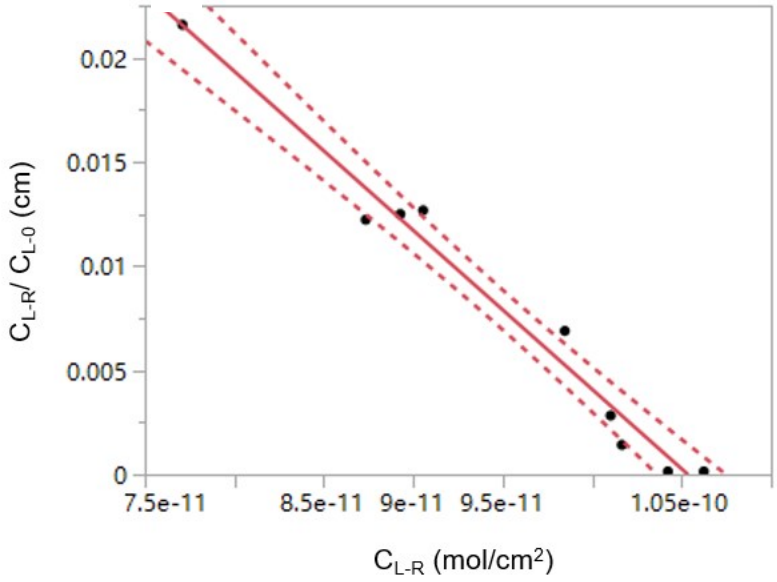

Figure 5. Scatchard plot of QCM-D data showing a linear fit with a 95% confidence interval. The slope from this model was used to estimate the binding constant (K_D).

The equilibrium dissociation constant (K_D) calculated based on the QCM-D Scatchard analysis was K_D = 1.3 ± 0.1 μM (standard error derived from the parameter estimates

of the linear fit shown in **Table S4**). The value for K_D is in good agreement with values found in literature for EF-hand peptides and lanthanides in solution (**Table S5**)[16-22, 24] indicating that the EF-hand loop I peptide maintains the ability to bind when surface-bound.

This study aims to determine the capacity for the EF-hand loop I peptide to bind to Ce^{3+} in solution and when surface-bound. Our CD results indicate that the EF-hand loop I peptide is capable of binding to Ce^{3+} in solution and this was supported by ITC data. Also, the secondary structure is important for binding Ce^{3+} as indicated by the CD analysis which shows binding is accompanied by a secondary structure change, and the scrambled controls which did not change structure in the presence of Ce^{3+}. The binding thermodynamics and structural changes are similar to other EF-hand peptides studied with lanthanides,[18, 19, 33] which supports an entropy-driven binding process.

The equilibrium binding constant of surface-bound peptide estimated from QCM-D is comparable to relevant literature examples using EF-hand peptides with other lanthanide ions (Supplemental Information **Table S5**),[16-22, 24] indicating that linking the peptide to a solid surface doesn't fatally hinder binding capabilities to Ce^{3+}. While investigation of the affinity of Ce^{3+} for the EF-hand peptide in this study (modified DKDGDGYISAAE), and the effect of tethering peptides to a solid substrate has been relatively unexplored in the literature, there are a few published studies for comparison. A particularly relevant study was conducted by Nitz *et al.* where a different EF-hand

peptide (YIDTNNDGWYEGDELLA) was found to have similar affinity for Ce^{3+} (K_D = 0.95 ± 0.05) in solution.[24] In another study, an EF-hand peptide of a different sequence was found to bind to Ce^{4+} with a K_D of 5.8 μM in solution.[16] Also, a peptide which incorporated the same binding sequence as this study (DKDGDGTITTKE) was found to bind to Tb^{3+} and La^{3+} with a K_D of 5 ± 1 and 12 ± 1 μM, respectively when grafted to domain 1 of a cell adhesion protein and tested in solution.[17] Broadly, our study implies that EF-hand peptides may be tethered to solid surfaces and retain their ability to bind ions. Future work may involve studying other EF-hand derivatives, other surfaces, other ions, and other pH conditions depending on the application. For example, the selectivity of the peptide may be characterized to assess its utility in lanthanide recovery, and other solid surfaces may be desired for materials synthesis.

4 Conclusions

An EF-hand loop I peptide derived from calmodulin (CGGGDKDGDGTITTKE) was shown to bind to cerium (III) ions. The binding in solution was accompanied by a change in secondary structure. The peptide formed a stable layer on gold, and had an affinity for cerium (III) ions when surface-bound. The peptide sequence was important for binding, as scrambled versions of the peptide did not bind as strongly when immobilized on gold, and did not change confirmation in the presence of cerium (III) ions in solution. Overall, these findings indicate that peptides derived from EF-hand motifs can be tethered to solid surfaces and retain the ability to bind to ions. Therefore, these peptides could be useful for future applications in materials engineering.

Acknowledgements

This work was supported by a Case Western Reserve University Glennan Fellowship. We thank CWRU for the opportunity to explore innovations in graduate teaching which manifested in this work. We also thank the United States Department of Agriculture (award number 2018-68011-28691) and the National Science Foundation (award number 1739473) which provided support for Zihang Su. We thank Yinghua Chen and the Protein Expression Purification and Crystallization Core facility (PEPCC) at the Case Western Reserve University Department of Physiology and Biophysics for assistance with ITC experiments, and Smarajit Bandyopadhyay at Department of Cellular and Molecular Medicine in Cleveland Clinic for his help with CD experiments. We also thank Sujay S. Ithychanda for the helpful discussions about ITC data analysis. Finally, Ziyue Yi came up with the original idea to explore cerium (III) ion binding to this peptide sequence and helped gather promising preliminary data.

Authors' Contributions

M. X. conducted all of the experiments shown, performed data analysis and was the primary author responsible for writing this manuscript. Z. S gathered QCM-D data in buffer, helped with QCM-D data analysis and interpretation, literature review and contributed to the editing of the manuscript. J. N. R. designed experiments, analyzed data, conducted statistical analysis and worked closely with the student team to write the manuscript.

References

1. Steinlechner, S.; Antrekowitsch, J., Potential of a Hydrometallurgical Recycling Process for Catalysts to Cover the Demand for Critical Metals, Like PGMs and Cerium. *Jom* **2015,** *67*, (2), 406-411.
2. Leung, P. K.; Ponce-de-León, C.; Low, C. T. J.; Shah, A. A.; Walsh, F. C., Characterization of a zinc–cerium flow battery. *Journal of Power Sources* **2011,** *196*, (11), 5174-5185.
3. Leung, P. K.; Mohamed, M. R.; Shah, A. A.; Xu, Q.; Conde-Duran, M. B., A mixed acid based vanadium–cerium redox flow battery with a zero-gap serpentine architecture. *Journal of Power Sources* **2015,** *274*, 651-658.
4. Le Toquin, R.; Cheetham, A. K., Red-emitting cerium-based phosphor materials for solid-state lighting applications. *Chemical Physics Letters* **2006,** *423*, (4), 352-356.
5. Komuro, N.; Mikami, M.; Shimomura, Y.; Bithell, E. G.; Cheetham, A. K., Synthesis, structure and optical properties of cerium-doped calcium barium phosphate – a novel blue-green phosphor for solid-state lighting. *Journal of Materials Chemistry C* **2015,** *3*, (1), 204-210.
6. Develos-Bagarinao, K., Nanostructured Cerium Oxide Films: Synthesis, Properties, and Applications. In *Oxide Thin Films, Multilayers, and Nanocomposites*, Mele, P.; Endo, T.; Arisawa, S.; Li, C.; Tsuchiya, T., Eds. Springer International Publishing: Cham, 2015; pp 213-235.
7. Castano, C. E.; O'Keefe, M. J.; Fahrenholtz, W. G., Cerium-based oxide coatings. *Curr. Opin. Solid State Mater. Sci.* **2015,** *19*, (2), 69-76.
8. Dhall, A.; Self, W., Cerium Oxide Nanoparticles: A Brief Review of Their Synthesis Methods and Biomedical Applications. *Antioxidants (Basel, Switzerland)* **2018,** *7*, (8), 97.
9. Comby, S.; Surender, E. M.; Kotova, O.; Truman, L. K.; Molloy, J. K.; Gunnlaugsson, T., Lanthanide-Functionalized Nanoparticles as MRI and Luminescent Probes for Sensing and/or Imaging Applications. *Inorg. Chem.* **2014,** *53*, (4), 1867-1879.
10. Montini, T.; Melchionna, M.; Monai, M.; Fornasiero, P., Fundamentals and Catalytic Applications of CeO2-Based Materials. *Chem. Rev.* **2016,** *116*, (10), 5987-6041.
11. Pollmann, K.; Kutschke, S.; Matys, S.; Kostudis, S.; Hopfe, S.; Raff, J., Novel Biotechnological Approaches for the Recovery of Metals from Primary and Secondary Resources. *Minerals* **2016,** *6*, (2), 54.
12. Galloway, J. M.; Staniland, S. S., Protein and peptide biotemplated metal and metal oxide nanoparticles and their patterning onto surfaces. *J. Mater. Chem.* **2012,** *22*, 12423-12434.
13. de la Rica, R.; Matsui, H., Applications of peptide and protein-based materials in bionanotechnology. *Chem Soc Rev* **2010,** *39*, (9), 3499-509.
14. Gifford, J. L.; Walsh, M. P.; Vogel, H. J., Structures and metal-ion-binding properties of the Ca2+-binding helix-loop-helix EF-hand motifs. *Biochem. J* **2007,** *405*, (2), 199-221.
15. Pidcock, E.; Moore, G. R., Structural characteristics of protein binding sites for

calcium and lanthanide ions. *J Biol Inorg Chem* **2001,** *6*, (5-6), 479-89.
16. Sirish, M.; Franklin, S. J., Hydrolytically active Eu(III) and Ce(IV) EF-hand peptides. *J. Inorg. Biochem.* **2002,** *91*, (1), 253-258.
17. Ye, Y.; Lee, H.-W.; Yang, W.; Shealy, S.; Yang, J. J., Probing Site-Specific Calmodulin Calcium and Lanthanide Affinity by Grafting. *J. Am. Chem. Soc.* **2005,** *127*, (11), 3743-3750.
18. Nakatsukasa, T.; Shiraishi, Y.; Negi, S.; Imanishi, M.; Futaki, S.; Sugiura, Y., Site-specific DNA cleavage by artificial zinc finger-type nuclease with cerium-binding peptide. *Biochem. Biophys. Res. Commun.* **2005,** *330*, (1), 247-252.
19. Welch, J. T.; Kearney, W. R.; Franklin, S. J., Lanthanide-binding helix-turn-helix peptides: Solution structure of a designed metallonuclease. *Proceedings of the National Academy of Sciences* **2003,** *100*, (7), 3725-3730.
20. Wojcik, J.; Goral, J.; Pawlowski, K.; Bierzynski, A., Isolated calcium-binding loops of EF-hand proteins can dimerize to form a native-like structure. *Biochemistry* **1997,** *36*, (4), 680-7.
21. Dadlez, M.; Goral, J.; Bierzynski, A., Luminescence of peptide-bound terbium ions. Determination of binding constants. *FEBS Lett.* **1991,** *282*, (1), 143-6.
22. Lopez, M. M.; Chin, D.-H.; Baldwin, R. L.; Makhatadze, G. I., The enthalpy of the alanine peptide helix measured by isothermal titration calorimetry using metal-binding to induce helix formation. *Proceedings of the National Academy of Sciences* **2002,** *99*, (3), 1298-1302.
23. Bentrop, D.; Bertini, I.; Cremonini, M. A.; Forsen, S.; Luchinat, C.; Malmendal, A., Solution structure of the paramagnetic complex of the N-terminal domain of calmodulin with two Ce3+ ions by 1H NMR. *Biochemistry* **1997,** *36*, (39), 11605-18.
24. Nitz, M.; Sherawat, M.; Franz, K. J.; Peisach, E.; Allen, K. N.; Imperiali, B., Structural Origin of the High Affinity of a Chemically Evolved Lanthanide-Binding Peptide. *Angewandte Chemie International Edition* **2004,** *43*, (28), 3682-3685.
25. Savage, A. C.; Pikramenou, Z., Peptide coated gold nanoparticles that bind lanthanide ions. *Chem Commun (Camb)* **2011,** *47*, (22), 6431-3.
26. Davies, A.; Lewis, D. J.; Watson, S. P.; Thomas, S. G.; Pikramenou, Z., pH-controlled delivery of luminescent europium coated nanoparticles into platelets. *Proceedings of the National Academy of Sciences of the United States of America* **2012,** *109*, (6), 1862-1867.
27. Liang, G.; Ye, D.; Zhang, X.; Dong, F.; Chen, H.; Zhang, S.; Li, J.; Shen, X.; Kong, J., One-pot synthesis of Gd3+-functionalized gold nanoclusters for dual model (fluorescence/magnetic resonance) imaging. *Journal of Materials Chemistry B* **2013,** *1*, (29), 3545-3552.
28. Ye, Y.; Lee, H.-W.; Yang, W.; Shealy, S. J.; Wilkins, A. L.; Liu, Z.-r.; Torshin, I.; Harrison, R.; Wohlhueter, R.; Yang, J. J., Metal binding affinity and structural properties of an isolated EF-loop in a scaffold protein. *Protein Engineering, Design and Selection* **2001,** *14*, (12), 1001-1013.
29. Malvern Instruments Ltd., MicroCal iTC200 system User Manual, 2014. http://www.isbg.fr/IMG/pdf/microcal-itc200-system-user-manual-malvern.pdf (accessed 4-8-19). In.

30. Ondaral, S.; Çelik, E.; Kurtuluş, O. Ç., The adsorption of phosphate-buffered saline to model films composed of nanofibrillated cellulose and gelatin. *Journal of Applied Biomaterials & Functional Materials* **2019,** *17*, (1), 2280800019826513.
31. Abellan, P.; Moser, T. H.; Lucas, I. T.; Grate, J. W.; Evans, J. E.; Browning, N. D., The formation of cerium(iii) hydroxide nanoparticles by a radiation mediated increase in local pH. *RSC Adv.* **2017,** *7*, (7), 3831-3837.
32. Chin, D.-H.; Woody, R. W.; Rohl, C. A.; Baldwin, R. L., Circular dichroism spectra of short, fixed-nucleus alanine helices. *Proceedings of the National Academy of Sciences* **2002,** *99*, (24), 15416.
33. Gifford, Jessica L.; Walsh, Michael P.; Vogel, Hans J., Structures and metal-ion-binding properties of the Ca²⁺-binding helix–loop–helix EF-hand motifs. *Biochem. J.* **2007,** *405*, (2), 199-221.
34. Lu, C. H.; Zhang, Y.; Tang, S. F.; Fang, Z. B.; Yang, H. H.; Chen, X.; Chen, G. N., Sensing HIV related protein using epitope imprinted hydrophilic polymer coated quartz crystal microbalance. *Biosens. Bioelectron.* **2012,** *31*, (1), 439-44.
35. Tai, D. F.; Jhang, M. H.; Chen, G. Y.; Wang, S. C.; Lu, K. H.; Lee, Y. D.; Liu, H. T., Epitope-cavities generated by molecularly imprinted films measure the coincident response to anthrax protective antigen and its segments. *Anal. Chem.* **2010,** *82*, (6), 2290-3.
36. Tai, D.-F.; Lin, C.-Y.; Wu, T.-Z.; Chen, L.-K., Recognition of Dengue Virus Protein Using Epitope-Mediated Molecularly Imprinted Film. *Anal. Chem.* **2005,** *77*, (16), 5140-5143.
37. Yan, B., *Analysis and Purification Methods in Combinatorial Chemistry*. John Wiley & Sons, Inc.: Hoboken, New Jersey, 2004.